Tumor and Stem Cell Biology

Cancer Research

mTOR Complex Component Rictor Interacts with PKCζ and Regulates Cancer Cell Metastasis

Fei Zhang, Xiaofang Zhang, Menghui Li, Peng Chen, Bin Zhang, Hua Guo, Wenfeng Cao, Xiying Wei, Xuchen Cao, Xishan Hao, and Ning Zhang

Abstract

Epidermal growth factor (EGF) mediates breast cancer cell chemotaxis and metastasis through mechanisms that involve the growth-regulatory mammalian target of rapamycin (mTOR) complex mTORC2, but the mechanisms involved remain obscure. Here, we report that the rapamycin-insensitive mTORC2 component protein Rictor is a critical mediator of metastasis in breast cancer cells. In patients with ductal carcinoma, Rictor expression was associated with increased lymph node metastasis. EGF induced translocation and colocalization of Rictor with protein kinase Cζ (PKCζ), a pivotal molecule in chemotaxis signaling. Further, Rictor coimmunoprecipitated with PKCζ in the absence of the mTORC2 complex. Small interfering RNA–mediated knockdown of Rictor inhibited EGF-induced PKCζ phosphorylation and translocation along with phosphorylation of the key F-actin binding protein cofilin. In parallel, Rictor knockdown reduced cellular chemotactic capacity and ablated pulmonary metastasis in a xenograft mouse model of breast cancer. Our findings identify Rictor as an important mediator of chemotaxis and metastasis in breast cancer cells. *Cancer Res; 70(22); 9360–70. ©2010 AACR.*

Introduction

The mammalian target of rapamycin (mTOR) plays a pivotal role in cell metabolism, growth, proliferation, and survival (1, 2). Based on their sensitivity to rapamycin treatment, mTOR nucleates two distinct multiprotein complexes, mTOR complex 1 (mTORC1) and mTOR complex 2 (mTORC2; refs. 3, 4). The mTORC1 complex is sensitive to rapamycin treatment and responds to a spectrum of intracellular and extracellular stimuli, such as growth factors, energy status, oxygen levels, amino acids, and inflammation (3, 5). On activation, mTORC1 promotes anabolic processes by limiting catabolic processes. The function and regulatory mechanisms of mTORC2 are less well defined. The mTORC2 complex is known to phosphorylate and activate Akt at Ser^{473} (6, 7). Moreover, preliminary studies have revealed that disruption of mTORC2 affects actin polymerization and perturbs cell morphology (4, 8). The rapamycin-insensitive companion of mTOR (Rictor) is a key component of mTORC2 and is required for mTORC2 function (4). Rictor interacts with two additional mTORC components, mammalian stress-activated protein kinase–interacting protein (mSIN1) and Protor1, to form a stable structure of the mTORC2 complex (7, 9, 10). Rictor may also function as a scaffold protein to mediate integrin-linked kinase activities (11). However, the role of Rictor in cancer cell chemotaxis and metastasis is largely unknown.

Metastasis is the major cause of mortality and morbidity among cancer patients. Chemotaxis is required for metastasis (12, 13). Epidermal growth factor (EGF)–induced chemotaxis mediates the detachment of cancer cells from primary sites and their subsequent intravasation into the circulation (14). Chemokine-induced chemotaxis mediates the extravasation of circulating tumor cells to secondary sites (12, 15). The molecular mechanism of chemotaxis has been extensively studied in *Dictyostelium discoideum*. On activation by an extracellular chemical gradient, cell surface receptors activate downstream heterotrimeric G proteins, phosphatidylinositol 3-kinases (PI3K), Cdc42, and Rac at the leading edge of a cell, inducing actin polymerization in lamellipodia to enable cell movement (16, 17). Meanwhile, PTEN and Rho are activated at the back of the cell, resulting in the formation of a contractile ring by myosin II (18). Phospholipase A2 and *pianissimo* (*Dictyostelium discoideum* homologue of Rictor) also regulate chemotaxis by unknown mechanisms in addition to the PI3K pathway (19, 20). In mammalian cells, paxillin and β_2 integrin are required for neutrophil chemotaxis (21), whereas integrin-mediated activation of focal adhesion kinase is essential for melanoma cell migration (22). PKCζ/PAR3/PAR6 regulates microtubule organization centers and is crucial for

Authors' Affiliation: Tianjin Medical University, Cancer Institute and Hospital, Research Center of Basic Medical Sciences, Key Laboratory of Breast Cancer Prevention and Therapy, Ministry of Education, Tianjin, China

Note: Supplementary data for this article are available at Cancer Research Online (http://cancerres.aacrjournals.org/).

F. Zhang and X. Zhang contributed equally to this work.

Corresponding Author: Ning Zhang, Tianjin Medical University, Research Center of Basic Medical Sciences and Cancer Institute and Hospital, Tianjin 300060, China. Phone: 86-13502179648; Fax: 86-22-23542068; E-mail: nzhangchina@yahoo.com.

doi: 10.1158/0008-5472.CAN-10-0207

astrocyte migration (23, 24). Understanding of eukaryotic cell chemotaxis has shed light on the investigation of cancer cell metastasis.

Chemotaxis of cancer cells is mediated by both chemokine and growth factor receptors (12, 25, 26). Our previous report has shown that protein kinase Cζ (PKCζ) is required for breast cancer cell chemotaxis (27). PKCζ is positively regulated by PDK1/Akt2 (28–30). Downregulation of PDK1 or Akt2 by small interfering RNA (siRNA) inhibits the metastasis of human breast cancer cells (MDA-MB-231) in a severe combined immunodeficient (SCID) mouse model (30, 31). Mechanistic studies suggest that PDK1/Akt2/PKCζ positively regulates cancer cell chemotaxis by activating cofilin/LIMK-mediated actin polymerization and integrin-mediated cell adhesion (27, 30, 31). We hypothesize that Rictor may regulate PKCζ in cancer cell chemotaxis and metastasis. In the current report, we investigate the expression pattern of Rictor in human breast cancer tissues and examine its role in chemotaxis and metastasis in a SCID mouse model.

Materials and Methods

Cells and cell culture

MDA-MB-231, T47D, and HEK293T cells were obtained from the American Type Culture Collection, where they were characterized by DNA profiling. MDA-MB-231 and T47D cells were cultured in RPMI 1640 supplemented with 10% (v/v) fetal bovine serum (FBS). HEK293T cells were grown in DMEM with 10% (v/v) FBS. All the cell lines were passaged for <6 months in this study.

Reagents, antibodies, and animals

RPMI 1640 was obtained from Invitrogen; FBS from Life Technologies; Lipofectamine 2000 from Invitrogen; micro-Boyden chambers from Neuroprobe; recombinant human EGF from R&D Systems; fibronectin (0.1%) from Sigma; enhanced chemiluminescence reagents from Pierce Biotechnology; Protease Inhibitor Cocktail tablets from Roche Diagnostics; antibodies against Akt, Akt2, phosphor-Akt (T308), phosphor-Akt (S473), and phospho-PKCz from Cell Signaling Technology; antibodies to Rictor from Bethyl Laboratories, Inc.; human Sin1 antibody from Millipore Corp.; Alexa Fluor 488–conjugated goat anti-rabbit IgG, Alexa Fluor 488–conjugated goat anti-mouse IgG, Alexa Fluor 647–conjugated goat anti-rabbit IgG, Alexa Fluor 647–conjugated goat anti-mouse IgG, and Alexa Fluor 568–phalloidin from Molecular Probes, Inc.; and SCID mice from Wei Tong Li Hua Experimental Animal Co. Ltd.

Immunohistochemical assay

Tissue microarrays were constructed with a Beecher Instruments Tissue Array as previously described (32). Archival paraffin blocks of invasive breast cancer cases were obtained from the Department of Breast Cancer, Tianjin Medical University Cancer Institute and Hospital. The antibodies and the dilution factors were as follows: Rictor (1:100), estrogen receptor (ER; 1:450; clone ID5 from DAKO), progesterone receptor (PR; 1:200; clone IA6 from DAKO), and human EGF receptor (EGFR) 2 (Her2/neu; 1:1,000; polyclonal from DAKO). Breast cancer cell lines MCF-7 and T47D were used as positive control for ER and PR, respectively. An ovarian cancer cell line, SK-OV-3, was used as a positive control for Her2/neu staining. PBS was used in the place of the primary antibodies in all negative controls of immunohistochemistry.

Plasmid construction, siRNA, and plasmid transfection

Full-length PKCζ was amplified by PCR and cloned into pFlag-CMV2 vector in the *Eco*RI and *Sal*I site. For transient transfections, three Stealth siRNAs against human Rictor (#1: 5′-AAAGGAUGCAGCCAUAUUCAUUAGG-3′; #2: 5′-AACAGUUCAAGGCUGCACUGGCUCG-3′; #3: 5′-GCAGCCTTGAACTGTTTAA-3′), two Sin1-specific Stealth siRNA duplexes (#1: 5′-GUCACUCUUUGUUCGAAUATT-3′; #2: 5′-GCAAUCACGACUAUAAACATT-3′), and a scrambled siRNA were synthesized by Invitrogen. BLOCK-iT Fluorescent Oligo was used to examine the transfection efficiency (Invitrogen). Seventy-two hours after transfections, cells were harvested and used for further experiments. For stable transfection, a siRNA expression plasmid containing #3 target sequence and a vector containing a scrambled sequence were obtained from Genechem Co. Stable transfectants were selected by using 800 μg/mL hygromycin B.

Reverse transcription-PCR, Western blotting, and isolation of membrane fractions

Reverse transcription-PCR (RT-PCR) and Western blotting assay were performed as described previously (27, 31). Briefly, PCRs were performed as follows: initial denaturation at 94°C for 5 minutes was followed by 30 cycles at 94°C for 30 seconds, 60°C for 30 seconds, and 72°C for 30 seconds. The PCR primers were as follows: Rictor (forward: 5′-TTTCGGGGATTTCTGGATG-3′, reverse: 5′-AAAGCCCAGTCTCATGACATT-3′) and β-actin (forward: 5′-GGCCGGGACCTGACTGACTAC-3′, reverse: 5′-GCCGCCAGACAGCACTGTGTT-3′). Cells were stimulated with 10 ng/mL EGF for 0 second, 30 seconds, 1 minute, 2 minutes, and 5 minutes, and phosphorylation of integrin β_1, cofilin, PKCζ, and Akt was analyzed. A protease inhibitor cocktail and phosphatase inhibitor cocktail were added to the cell lysis buffer before protein extraction.

To isolate membrane fraction, cells were resuspended in 500 μL of subcellular fractionation buffer (250 mmol/L sucrose, 20 mmol/L HEPES, 10 mmol/L KCl, 1.5 mmol/L $MgCl_2$, 1 mmol/L EDTA, 1 mmol/L EGTA, and protein inhibitor cocktail) at 4°C and lysed through a 25-gauge needle 10 times using a 1-mL syringe. Lysates were centrifuged at 1,000 × *g* for 10 minutes to remove nuclear pellet, and supernatants were centrifuged again at 100,000 × *g* for 1 hour. The supernatant was the cytosol fraction. The pellet, the membrane fraction, was washed and resuspended in the lysis buffer with 10% glycerol and 0.2% SDS for further analysis.

Cell proliferation, chemotaxis, adhesion, and wound-healing assay

Cell proliferation assay was done as described previously (33). Briefly, cells were plated in 96-well plates. Twenty microliters of the stock MTT solution (5 mg/mL) in PBS were

added to each well at different times and incubated for 4 hours at 37°C. Cell activity was calculated by the absorbency at 570 nm. Chemotaxis assays were performed by using micro-Boyden chambers as described previously (27). After 3 hours of chemotaxis assay in a 37°C humidified incubator for 3 hours, the membranes were fixed and stained. The number of migrating cells was counted by light microscopy at 400× (high-powered field). In adhesion assays, cells were suspended in serum-free medium at a final concentration of 4×10^5/mL and incubated at 37°C for 30 minutes. The suspension with or without 10 ng/mL EGF was added into a 3.5-mm dish containing fibronectin-coated glass coverslips. After an incubation of 5, 15, and 30 minutes, the coverslips were washed with PBS and fixed. The attached cells were counted under a light microscope at 200×. For wound-healing assays, cells were seeded in six-well plates and grown until 100% confluence (31). After making a straight scratch by using a pipette tip, cells were incubated in a minimum medium (containing 0.5% FBS) in a 37% humidified incubator for 0, 3, 6, 9, and 12 hours and the wound distances were measured under a light microscope.

Immunofluorescence confocal microscopy

Confocal microscopy was performed as described previously with minor modification (27). Briefly, cells were plated in 12-well plates containing sterile coverslips, allowed for 24-hour growth, and starved in serum-free RPMI 1640 for at least 3 hours. After stimulation with 10 ng/mL EGF for 10 minutes at 37°C, cells were fixed with 4% paraformaldehyde, quenched with 50 mmol/L NH_4Cl, permeabilized in 0.2% Triton X-100 in PBS, and blocked in 3% bovine serum albumin. Cells were stained with anti-Rictor and/or anti-PKCζ antibodies and probed with either an Alexa Fluor 488– or an Alexa Fluor 647–conjugated secondary antibody. Coverslips were mounted and visualized with confocal laser scanning microscopy (Leica TCS SP5). For wound-healing assays, cells were allowed to migrate for 6 hours, then fixed with 4% paraformaldehyde, and stained with anti-Rictor and anti-PKCζ antibodies. Colocalization efficiency was calculated through ImageJ software (NIH, Bethesda, MD). The plasma membrane regions of the cell or full image were selected as the region of interest to quantify the colocalization efficiency. Twenty-five images were analyzed.

Coimmunoprecipitation

Coimmunoprecipitation was performed as described with minor modification (4). Briefly, cells were seeded in 10-cm dishes and grown to 80% to 90% confluence. After 4 hours of serum starvation, cells were either left unstimulated or stimulated with 10 ng/mL EGF for 5 minutes. After washing three times with PBS, cells were lysed in 1 mL of ice-cold cell lysis buffer (40 mmol/L HEPES, 120 mmol/L NaCl, 1% Triton X-100 or 0.3% CHAPS, 10 mmol/L pyrophosphate, 10 mmol/L glycerophosphate, 50 mmol/L NaF, 1.5 mmol/L Na_3VO_4,

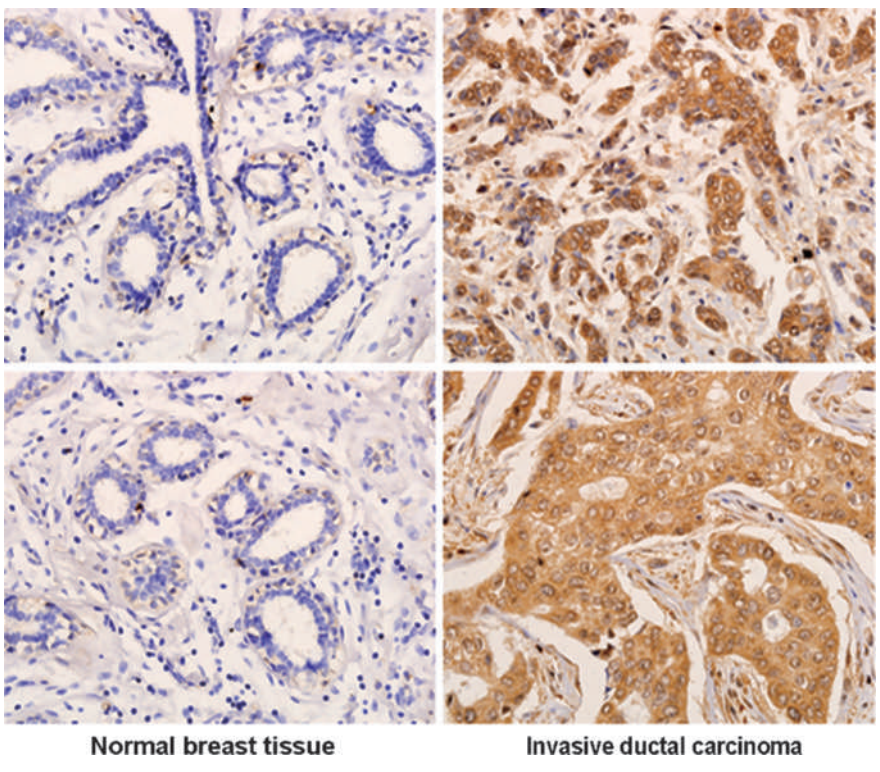

Figure 1. Rictor expression is elevated in invasive ductal carcinoma tissues. Immunohistochemical analysis of breast invasive ductal carcinoma tissues and normal breast tissues. Sections were stained with an anti-Rictor antibody.

1 mmol/L EDTA, and complete protease inhibitor cocktail, pH 7.5) on ice for 30 minutes. After centrifugation at 12,000 × *g* for 15 minutes, supernatants were removed and precleared by adding 50 μL of protein A for an hour. Supernatants were immunoprecipitated by using anti-PKCζ or anti-Rictor antibodies. The immunocomplex was captured by adding 50 μL of protein A and subjected to Western blotting analysis.

In vivo spontaneous metastasis assay

Metastasis assays were performed as described previously (31). Briefly, siRictor and control cells were grown until the log phase, trypsinized, and washed four times with serum-free medium. Four-week-old female SCID mice were injected s.c. into the mammary fat pads with 2×10^6 cells ($n = 10$ per group). Tumor diameters were measured every week after injection of cancer cells. After 6 or 9 weeks, the mice were sacrificed, the tumors were isolated, and tumor weights were measured. To examine spontaneous metastasis, the lungs were fixed with formalin and embedded in paraffin. Serial sections and H&E staining were performed to detect lung micrometastasis.

Results

Expression of Rictor is correlated with lymph node metastasis in invasive ductal carcinoma patients

Invasive ductal carcinoma accounts for >80% of breast cancer incidents in China.[1] The expression of Rictor was examined by immunohistochemistry in 39 pairs of invasive ductal carcinoma tissues, including tumors and tumor-associated tissues. Positive staining was detected in 25 tumor samples but only in three tumor-associated tissues, suggesting that expression of Rictor is elevated during tumorigenesis (Fig. 1). Indeed, Rictor was observed at a significantly higher rate in tumor samples than in tumor-associated tissue ($P < 0.001$). Further statistical analysis revealed that Rictor expression was detected in 24 of 26 lymph node metastasis cases ($P = 0.003$; Table 1). In 13 non–lymph node metastasis cases, only one tumor tissue was positive. These results strongly suggest that expression of Rictor is associated with metastasis, either as a cause or as a consequence. Taken together, these results indicate that the expression of Rictor is elevated in breast cancer tissues and is associated with lymph node metastasis.

Table 1. Correlation of Rictor expression with clinicopathologic parameters and other biomarkers

Parameters/markers	Total	Positive	%	*P*
Menopausal				
Premenopausal	21	12	57.1	0.341
Postmenopausal	18	13	72.2	
Tumor size (cm)				
<2	7	5	71.4	0.666
>2	32	20	62.5	
Lymph node status				
Negative	13	1	0.07	0.003
Positive	26	24	92.3	
Histologic grade				
G1	13	9	69.2	0.519
G2	22	14	63.6	
G3	4	2	50.0	
ER status				
Negative	16	7	43.8	0.027
Positive	23	18	78.3	
PR status				
Negative	18	10	55.6	0.316
Positive	21	15	71.4	
Her2/neu protein				
Negative	29	16	55.2	0.049
Positive	10	9	90.0	

Knockdown of Rictor by siRNA inhibits cancer cell migration

We hypothesize that Rictor plays an important role in metastasis by regulating cancer cell chemotaxis. To test this hypothesis, three independent siRNAs (#1, #2, and #3 siRNA) were designed to target Rictor, and a scrambled sequence was used as a control. Transient transfection with each of three siRNA specifically downregulated Rictor expression in MDA-MB-231 cells, whereas transfection with the scrambled sequence did not (Fig. 2A). Western blotting analysis showed a block at EGF-induced Akt phosphorylation at Ser^{473}, indicating that the function of Rictor was inhibited in siRictor cells (Fig. 2A; refs. 6, 34). One of the siRNA sequences was selected to generate stable clones of Rictor knockdown cells. Three representative clones (clones 4, 11, and 15) were used in the analysis (Fig. 2B). All three clones had similar phenotypes; thus, we choose to present the results from clone 4 as the representative, which is designated as siRictor. A scrambled sequence was used to replace the siRNA sequence in the expressing vector and transfected to generate a stable cell line, designated as Scrambled (Scr). Scr cells showed a level of Rictor comparable with their parental cells, MDA-MB-231, suggesting that the expressing vector did not interfere with Rictor expression. MTT assays revealed that siRictor clones showed an average reduction of 15% in cell proliferation *in vitro*, which did not interfere with the following assays of chemotaxis properties (Fig. 2C). Next, we examined siRictor cells by using a scratch assay in a serum-free medium. As shown in Fig. 2D, siRictor cells failed to fill the gap 12 hours after the scratch, suggesting that directional migration was impaired. Taken together, we were able to downregulate Rictor levels by siRNA and siRictor cells had a defect in directional migration.

[1] Unpublished data.

Knockdown of Rictor severely impaired chemotaxis of human breast cancer cells

Our previous report has shown that PKCζ mediates EGF-induced chemotaxis by regulating actin polymerization (27, 35). As shown in Fig. 3A, knockdown of Rictor or PKCζ by transient transfection inhibited EGF-induced chemotaxis of MDA-MB-231 cells (Fig. 3A). All three stable siRNA clones were also defective in chemotaxis (Fig. 3A). Downregulation of Rictor or PKCζ in T47D, another human breast cancer cell line, also impaired EGF-induced chemotaxis (Supplementary Fig. S1). Both cell adhesion and actin polymerization are required for a robust chemotaxis (36, 37). As shown in Fig. 3B and C, EGF-induced cell adhesion and phosphorylation of integrin β_1 was impaired in siRictor cells. Cofilin, an actin associate protein, plays an important role in actin polymerization (27). As shown in Fig. 3D, EGF-induced cofilin phosphorylation was inhibited in Rictor knockdown cells. Moreover, EGF-induced actin polymerization was altered (Supplementary Fig. S2). Taken together, our results indicate that Rictor regulates EGF-induced human breast cancer cell chemotaxis, probably by mediating cell adhesion and actin polymerization.

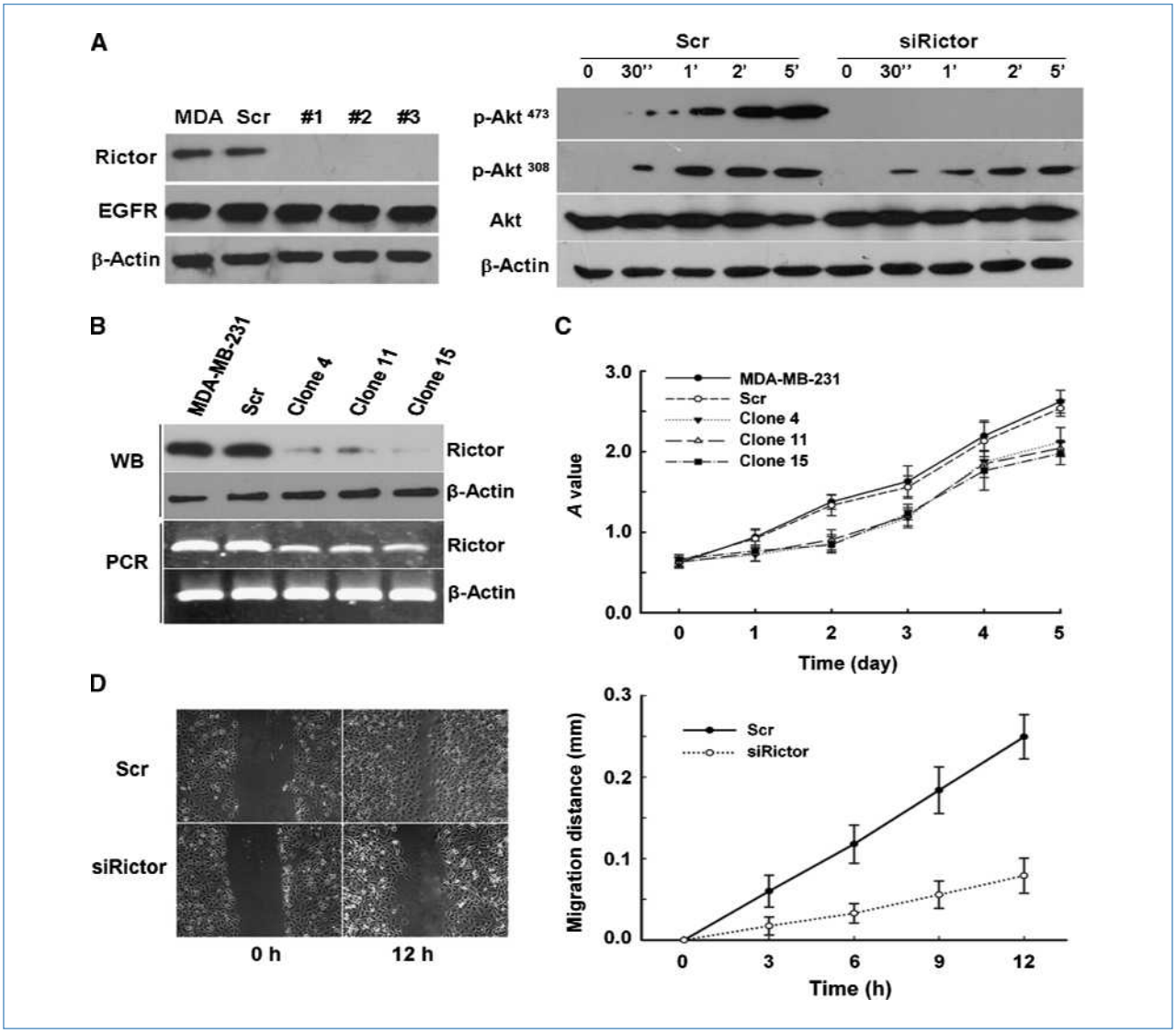

Figure 2. Knockdown of Rictor expression by siRNA inhibited human breast cancer cell migration. A, downregulation of Rictor inhibits phosphorylation of Akt at Ser^{473} site. Left, Western blotting analysis of Rictor and EGFR expression in MDA-MB-231 cells and MDA-MB-231 cells transfected with three sets of Stealth siRNA-targeting Rictor (#1, #2, and #3) and with a scrambled siRNA as a control (Scr). β-Actin was used as a loading control. Right, Western blotting analysis of EGF-induced phosphorylation of Akt at Ser^{473} and Thr^{308} sites in cell lysate. B, Western blotting (WB) and RT-PCR analysis of Rictor expression in MDA-MB-231 cells, Scr cells, and three stable Rictor knockdown clones. C, cell proliferation activity was impaired in siRictor cells. Points, mean ($n = 3$); bars, SD. Statistical analysis was performed by a one-way ANOVA ($P < 0.05$ versus Scr cells). D, wound-healing assay of Scr and siRictor cells (clone 4). The gap distance on Scr and siRictor cell (clone 4) monolayer was measured at 0, 3, 6, 9, and 12 h after scratches were created.

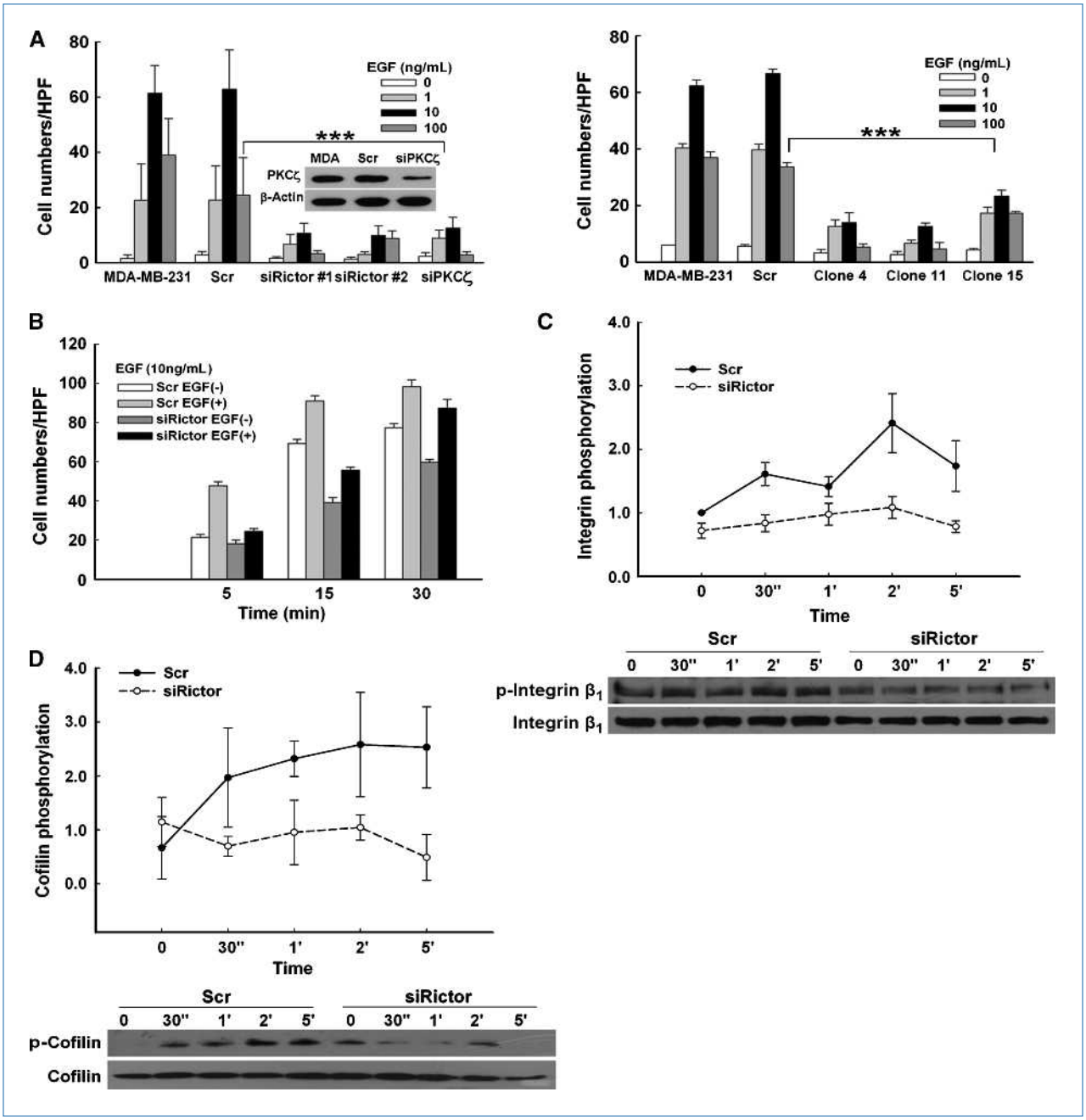

Figure 3. Downregulation of Rictor severely impaired chemotaxis of human breast cancer cells. A, chemotaxis analysis of Rictor or PKCζ knockdown cells. Left, comparison of chemotaxis of MDA-MB-231 cells, cells transfected with a scramble siRNA, and cells transfected with two different siRNA-targeting Rictor (#1 and #2) and with siRNA-targeting PKCζ. Right, chemotaxis assays of three stable Rictor knockdown clones. B, EGF-induced cell adhesion was decreased in siRictor cells (stable clone 4). C, Western blotting analysis of EGF-induced phosphorylation of integrin β_1 in total cell lysate from Scr and siRictor cells (stable clone 4). Points, mean of three independent experiments; bars, SD. Statistical analysis was performed by a two-way ANOVA ($P < 0.0001$). D, Western blotting analysis of EGF-induced phosphorylation of cofilin in total cell lysate from Scr and siRictor cells (stable clone 4). Points, mean of three independent experiments; bars, SD. Statistical analysis was performed by a two-way ANOVA ($P < 0.0001$).

Rictor colocalized with PKCζ at the leading edge of the cell and regulated its activation

Next, we investigated the possibility that Rictor interacts with PKCζ in cancer cells. Confocal microscopy analysis showed that both Rictor and PKCζ were distributed in the cytosol of resting cells, consistent with previous reports (Fig. 4A; ref. 27). On stimulation with 10 ng/mL EGF for 10 minutes, both PKCζ and Rictor proteins were enriched along the plasma membrane, suggesting activation of both proteins (Fig. 4A). Rictor colocalized with PKCζ on the

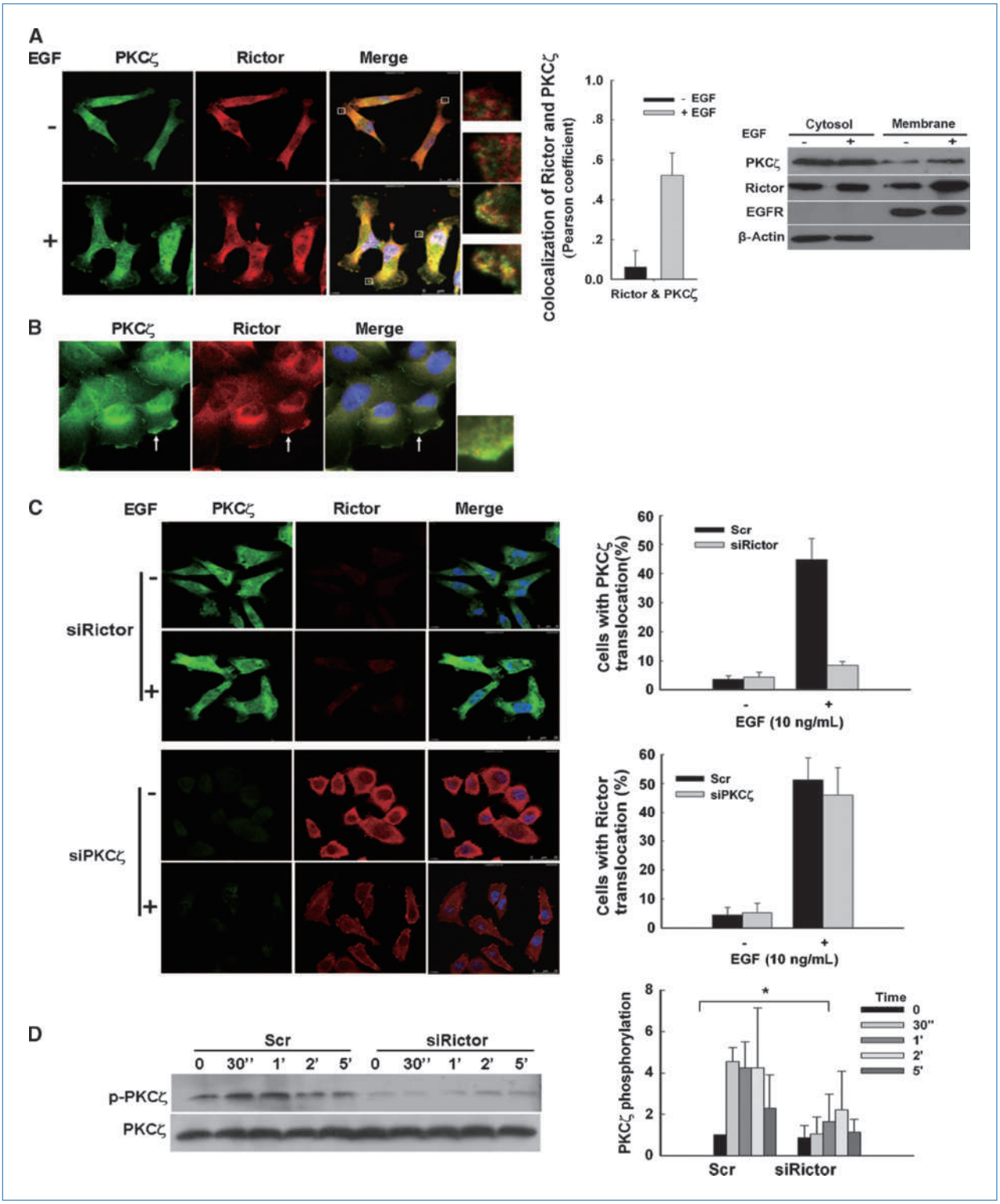

Figure 4. Rictor colocalized with PKCζ at the leading edge of a cell and regulated its activation. A, Rictor colocalized with PKCζ on the plasma membrane. Left, confocal microscopic analysis of PKCζ with Rictor in the presence or absence of EGF stimulation (10 ng/mL, 10 min); right, Western blotting analysis of Rictor and PKCζ translocation to the plasma membrane in MDA-MB-231 cells on stimulation with 10 ng/mL EGF for 10 min. B, PKCζ colocalized with Rictor at the leading edge of migrating cells in a scratch assay. C, knockdown of Rictor impaired EGF-induced membrane translocation of PKCζ, but knockdown of PKCζ has no effect on EGF-induced membrane translocation of Rictor. D, Western blotting analysis of EGF-induced phosphorylation of PKCζ in total cell lysate from Scr and siRictor cells (stable clone 4). Three independent Western blotting analyses were analyzed by a two-way ANOVA ($P = 0.0015$).

plasma membrane as determined by image analysis through ImageJ software (Fig. 4A). Western blotting analysis showed EGF-induced increase of PKCζ and Rictor in plasma membrane fraction, further confirming the observation from confocal microscopy analysis (Fig. 4A). Next, scratch assays revealed that both Rictor and PKCζ proteins were enriched in the front of migratory cells along with PKCζ (Fig. 4B).

The translocation of both Rictor and PKCζ was analyzed in knockdown cells. Knockdown of Rictor inhibited EGF-induced translocation of PKCζ (Fig. 4C; Supplementary Fig. S3A). Furthermore, EGF-induced phosphorylation of PKCζ was reduced in siRictor cells (Fig. 4D). In siPKCζ cells, EGF still induced membrane translocation of Rictor (Fig. 4C; Supplementary Fig. S3B). Taken together, the results suggest that Rictor may act upstream of PKCζ and is required for full activation of PKCζ.

Rictor interacted with PKCζ in the absence of mTOR

The interaction between Rictor and PKCζ was examined by coimmunoprecipitation assays. In a lysis buffer containing 0.3% CHAPS to preserve the integrity of mTORC2 complex, Rictor coprecipitated with mTOR and PKCζ, whereas PKCζ only coprecipitated with Rictor but not with mTOR (Fig. 5A). In a lysis buffer containing 1% Triton X-100, which disrupted mTORC2, Rictor still coprecipitated with PKCζ, suggesting that mTOR2 complex was not required for the interaction between Rictor and PKCζ. Rictor also coimmunoprecipitated with Flag-PKCζ overexpressed in HEK293T cells (Supplementary Fig. S4).

Sin1 is an essential component of mTOR2 complex (7, 10). Knockdown of Sin1 disrupted the function of mTORC2 (Fig. 5C). However, Rictor still coimmunoprecipitated with PKCζ in Sin1 knockdown cells (Fig. 5D). Furthermore, Sin1 knockdown cells showed robust chemotaxis properties (Supplementary Fig. S5). Thus, results suggest that interaction between Rictor and PKCζ does not require the integrity of mTORC2.

Downregulation of Rictor by siRNA inhibited tumor growth and metastasis of human breast tumors

The metastasis properties of siRictor cells were analyzed *in vivo* through a xenograft transplant model in SCID mice. Scr and siRictor cells were implanted into the mammary fat pads of SCID mouse. After 6 weeks, a significant reduction in tumor growth was detected in mice with transplanted siRictor cells, suggesting that Rictor plays an important role in tumor growth *in vivo* (Fig. 6A). Lung metastasis of human breast cancer cells was evaluated through staining with H&E. No tumor foci were detected

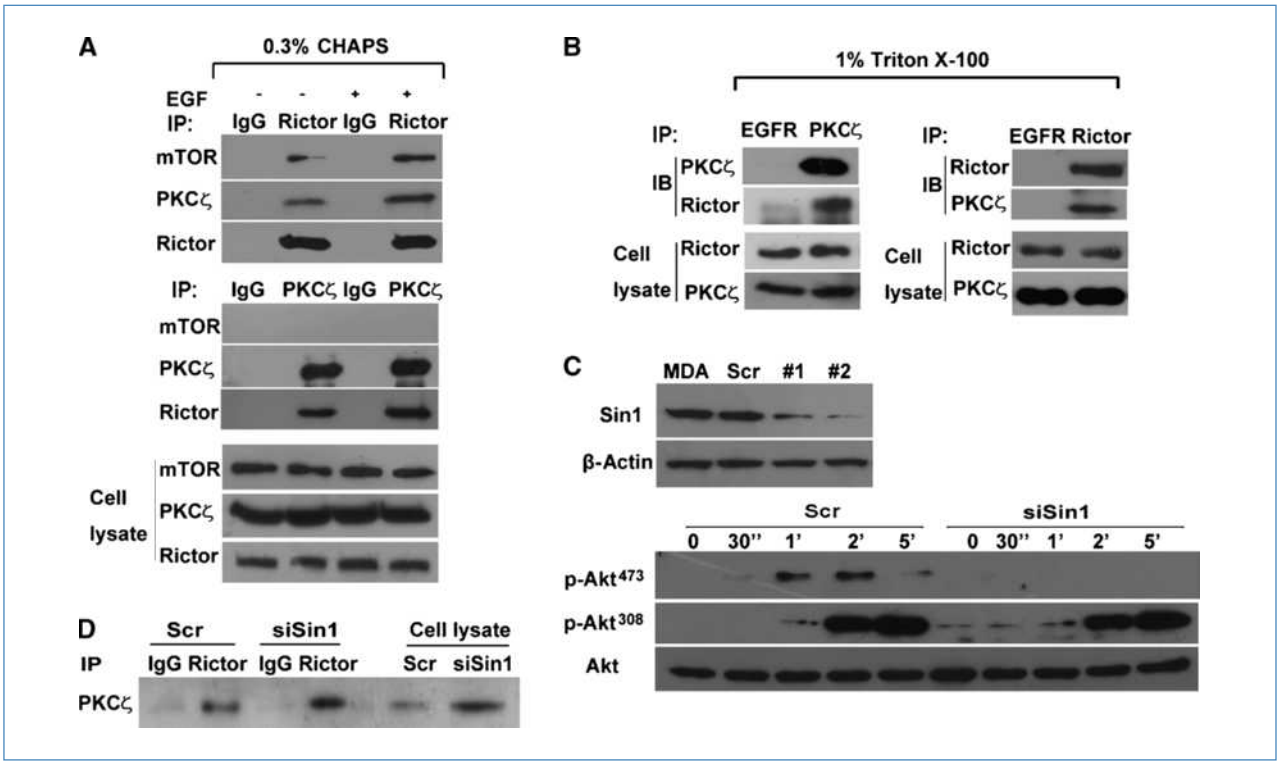

Figure 5. Endogenous Rictor coimmunoprecipitated with PKCζ independent of mTORC2. A, coimmunoprecipitation of endogenous Rictor or PKCζ in 0.3% CHAPS lysis buffer. Nonimmune IgG was used as a control. B, coimmunoprecipitation of endogenous Rictor or PKCζ in 1% Triton X-100 lysis buffer. EGFR was used as a control. C, downregulation of Sin1 inhibits phosphorylation of Akt at Ser^{473} site. Top, Western blotting analysis of MDA-MB-231 cells transfected with two sets of siRNA-targeting Sin1; bottom, Western blotting analysis of EGF-induced phosphorylation of Akt at Ser^{473} and Thr^{308} sites in Scr and Sin1 knockdown cells. D, endogenous Rictor immunoprecipitated with PKCζ in Sin1 knockdown cells.

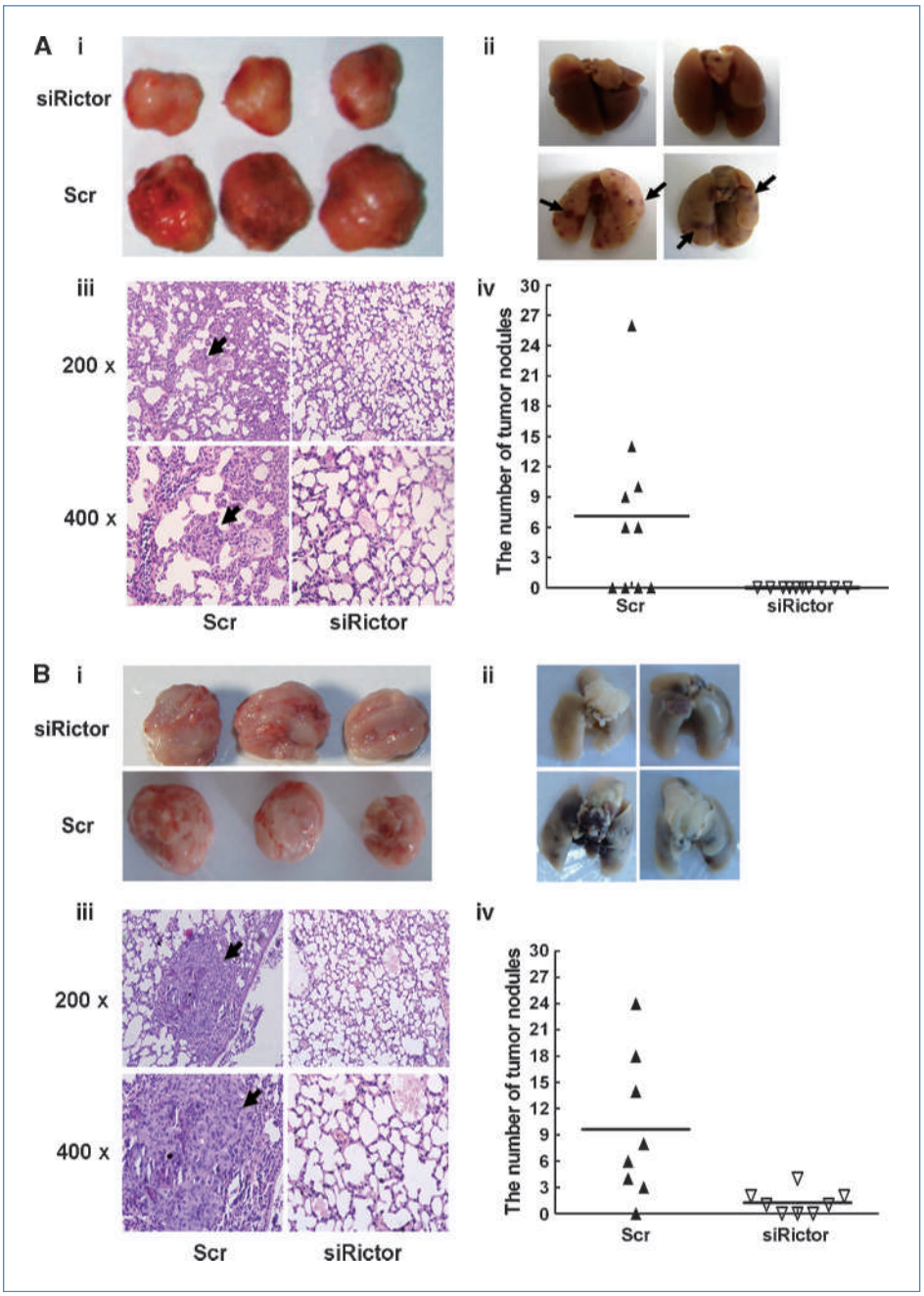

Figure 6. Downregulation of Rictor inhibited metastasis of human breast tumors. A, comparison of tumor size and spontaneous lung metastasis in SCID mice implanted with Scr or siRictor cells (stable clone 4) for 6 wk. i, images of representative primary tumors. ii, images of representative lung metastasis. iii, human tumor foci on mouse lungs were visualized by H&E staining. iv, the number of lung metastases was counted and plotted (n = 10). B, comparison of tumor size and spontaneous lung metastasis in Scr (6 wk) and siRictor cells (9 wk, mixture of clones 4, 11, and 15) of transplanted SCID mice. Each group contained eight mice (n = 8).

in the lungs of siRictor-implanted mice. In contrast, extensive tumor foci were found in 6 of 10 mice transplanted with scrambled siRNA controls. To rule out the influence of tumor growth in metastasis assays, during the second sets of experiments, mice implanted with siRictor cells were allowed to grow to 9 weeks, 3 weeks longer than those implanted with control cells. As shown in Fig. 6B, the sizes of primary tumors from siRictor-implanted mice were slightly larger than those from control mice. Lung metastasis from siRictor cells was still significantly lower than that from control cells. Thus, our results clearly indicate that Rictor is required for metastasis of human breast cancers *in vivo*.

Discussion

Our results support the hypothesis that Rictor plays an important role in cancer cell metastasis. Pathologic investigation of patient tissues indicates that Rictor is expressed in ~64% of ductal carcinoma tumor samples and only 7% in

tumor-associated tissues, suggesting that the majority of cancer patients have enhanced Rictor expression within their tumors. Microscopic analysis of the 7% of Rictor-positive tumor-associated tissues by pathologists revealed changes in cell morphology, suggesting that these tissues may be in the early stages of tumorigenesis. The most striking evidence to support the premise that Rictor plays a role in metastasis involves the analysis of lymph nodes from metastasis patients, which are 92% Rictor-positive compared with <10% Rictor-positive samples from non–lymph node metastasis patients. In animal experiments, downregulation of Rictor through siRNA inhibited metastasis of human breast cancer cells to the lungs of SCID mice, providing molecular evidence that Rictor is required for spontaneous metastasis of human breast cancer cells *in vivo*.

Previous studies have suggested that knockdown of Rictor impairs actin cytoskeleton structure (4, 8). Our current study indicates that Rictor colocalizes with PKCζ at the leading edges of cells. Endogenous Rictor interacts with PKCζ in the absence of mTORC2 complex. Knockdown of Rictor inhibited PKCζ translocation and full activation. In siRictor cells, EGF-induced cofilin phosphorylation was impaired. Thus, our results suggest a novel mechanism of Rictor in chemotaxis of human cancer cells. Knockdown of Rictor expression inhibits PKCα activity in HeLa and glioma cells (4, 38). PKCα also regulates actin structure in these cells. However, in both human breast cancer cells and leukocytes, treatment with inhibitors of classic PKC does not inhibit chemotaxis (27). Thus, the function of PKCα in chemotaxis may be cell type specific.

Our results suggest that Rictor interacts and regulates PKCζ activation independent of mTORC2. Rictor was initially identified as a scaffold protein for the mTORC2 complex (4). Knockdown of Sin1, an essential component of mTORC2, does not interfere with EGF-induced chemotaxis and coimmunoprecipitation between Rictor and PKCζ, suggesting that mTORC2 may not play a role in regulating EGF-induced cancer cell chemotaxis. A report by McDonald and colleagues (11) suggests that Rictor may also form a complex with other proteins, such as integrin-linked kinase. Thus, it is plausible that Rictor as a general scaffold protein, but not mTORC2, is required for EGF-induced chemotaxis of cancer cells.

Identifying the role of Rictor in cancer cell chemotaxis and metastasis provides a novel molecule for cancer diagnosis, prognosis, and therapy. Immunohistochemical assays suggest that Rictor may be a novel biomarker for breast cancer metastasis. In addition, the expression of Rictor is closely linked with papillary renal cell carcinoma, a highly metastatic cancer.[1] In lung cancer patients, expression of Rictor is inversely linked with 3-year surviving rate.[2] Our results also suggest that Rictor can be used as a novel drug target to treat cancer metastasis. In both *Saccharomyces cerevisiae* and *D. discoideum*, cells are viable on disruption of *rictor* gene, suggesting that targeting Rictor will not cause severe cytotoxicity (20). Thus, Rictor may be used as a novel biomarker or as a target to develop novel metastasis therapy.

Disclosure of Potential Conflicts of Interest

No potential conflicts of interest were disclosed.

Acknowledgments

We thank Dr. Jiming Wang and David Blake for critical reading of the manuscript, Dr. Yi Yang for technique assistance with confocal microscopy, and Dr. Fenglin Zang for immunohistochemical evaluation.

Grant Support

NFSC grant 30772529 and 973 program grants 2011CB933100 and 2010CB933900.

The costs of publication of this article were defrayed in part by the payment of page charges. This article must therefore be hereby marked *advertisement* in accordance with 18 U.S.C. Section 1734 solely to indicate this fact.

Received 01/18/2010; revised 09/02/2010; accepted 09/02/2010; published OnlineFirst 10/26/2010.

[2] Unpublished data.

References

1. Guertin DA, Sabatini DM. Defining the role of mTOR in cancer. Cancer Cell 2007;12:9–22.
2. Wullschleger S, Loewith R, Hall MN. TOR signaling in growth and metabolism. Cell 2006;124:471–84.
3. Kim DH, Sarbassov DD, Ali SM, et al. mTOR interacts with raptor to form a nutrient-sensitive complex that signals to the cell growth machinery. Cell 2002;110:163–75.
4. Sarbassov DD, Ali SM, Kim DH, et al. Rictor, a novel binding partner of mTOR, defines a rapamycin-insensitive and raptor-independent pathway that regulates the cytoskeleton. Curr Biol 2004;14:1296–302.
5. Lee DF, Kuo HP, Chen CT, et al. IKKβ suppression of TSC1 links inflammation and tumor angiogenesis via the mTOR pathway. Cell 2007;130:440–55.
6. Sarbassov DD, Guertin DA, Ali SM, Sabatini DM. Phosphorylation and regulation of Akt/PKB by the rictor-mTOR complex. Science 2005;307:1098–101.
7. Jacinto E, Facchinetti V, Liu D, et al. SIN1/MIP1 maintains rictor-mTOR complex integrity and regulates Akt phosphorylation and substrate specificity. Cell 2006;127:125–37.
8. Jacinto E, Loewith R, Schmidt A, et al. Mammalian TOR complex 2 controls the actin cytoskeleton and is rapamycin insensitive. Nat Cell Biol 2004;6:1122–8.
9. Pearce LR, Huang X, Boudeau J, et al. Identification of Protor as a novel Rictor-binding component of mTOR complex-2. Biochem J 2007;405:513–22.
10. Frias MA, Thoreen CC, Jaffe JD, et al. mSin1 is necessary for Akt/PKB phosphorylation, and its isoforms define three distinct mTORC2s. Curr Biol 2006;16:1865–70.
11. McDonald PC, Oloumi A, Mills J, et al. Rictor and integrin-linked kinase interact and regulate Akt phosphorylation and cancer cell survival. Cancer Res 2008;68:1618–24.
12. Muller A, Homey B, Soto H, et al. Involvement of chemokine receptors in breast cancer metastasis. Nature 2001;410:50–6.
13. Balkwill F. Cancer and the chemokine network. Nat Rev Cancer 2004;4:540–50.
14. Xue C, Wyckoff J, Liang F, et al. Epidermal growth factor receptor overexpression results in increased tumor cell motility *in vivo* coordinately with enhanced intravasation and metastasis. Cancer Res 2006;66:192–7.

15. Chambers AF, Groom AC, MacDonald IC. Dissemination and growth of cancer cells in metastatic sites. Nat Rev Cancer 2002;2: 563–72.
16. Iglesias PA, Devreotes PN. Navigating through models of chemotaxis. Curr Opin Cell Biol 2008;20:35–40.
17. Veltman DM, Keizer-Gunnik I, Van Haastert PJ. Four key signaling pathways mediating chemotaxis in *Dictyostelium discoideum*. J Cell Biol 2008;180:747–53.
18. Li Z, Dong X, Wang Z, et al. Regulation of PTEN by Rho small GTPases. Nat Cell Biol 2005;7:399–404.
19. Kolsch V, Charest PG, Firtel RA. The regulation of cell motility and chemotaxis by phospholipid signaling. J Cell Sci 2008;121:551–9.
20. Chen MY, Long Y, Devreotes PN. A novel cytosolic regulator, Pianissimo, is required for chemoattractant receptor and G protein-mediated activation of the 12 transmembrane domain adenylyl cyclase in *Dictyostelium*. Genes Dev 1997;11:3218–31.
21. Fuortes M, Jin WW, Nathan C. β2 Integrin-dependent tyrosine phosphorylation of paxillin in human neutrophils treated with tumor necrosis factor. J Cell Biol 1994;127:1477–83.
22. Mostafavi-Pour Z, Askari JA, Parkinson SJ, Parker PJ, Ng TT, Humphries MJ. Integrin-specific signaling pathways controlling focal adhesion formation and cell migration. J Cell Biol 2003; 161:155–67.
23. Etienne-Manneville S, Hall A. Integrin-mediated activation of Cdc42 controls cell polarity in migrating astrocytes through PKCζ. Cell 2001;106:489–98.
24. Etienne-Manneville S, Manneville JB, Nicholls S, Ferenczi MA, Hall A. Cdc42 and Par6-PKCζ regulate the spatially localized association of Dlg1 and APC to control cell polarization. J Cell Biol 2005;170:895–901.
25. Kakinuma T, Hwang ST. Chemokines, chemokine receptors, and cancer metastasis. J Leukoc Biol 2006;79:639–51.
26. Ben-Baruch A. Organ selectivity in metastasis: regulation by chemokines and their receptors. Clin Exp Metastasis 2008;25:345–56.
27. Sun R, Gao P, Chen L, et al. Protein kinase Cζ is required for epidermal growth factor-induced chemotaxis of human breast cancer cells. Cancer Res 2005;65:1433–41.
28. Chou MM, Hou W, Johnson J, et al. Regulation of protein kinase Cζ by PI 3-kinase and PDK-1. Curr Biol 1998;8:1069–77.
29. Le Good JA, Ziegler WH, Parekh DB, Alessi DR, Cohen P, Parker PJ. Protein kinase C isotypes controlled by phosphoinositide 3-kinase through the protein kinase PDK1. Science 1998;281:2042–5.
30. Wang J, Wan W, Sun R, et al. Reduction of Akt2 expression inhibits chemotaxis signal transduction in human breast cancer cells. Cell Signal 2008;20:1025–34.
31. Liu Y, Wang J, Wu M, et al. Down-regulation of 3-phosphoinositide-dependent protein kinase-1 levels inhibits migration and experimental metastasis of human breast cancer cells. Mol Cancer Res 2009;7: 944–54.
32. Cao W, Zhang B, Liu Y, et al. High-level SLP-2 expression and HER-2/neu protein expression are associated with decreased breast cancer patient survival. Am J Clin Pathol 2007;128:430–6.
33. Zhang F, Zhang L, Zhang B, et al. Anxa2 plays a critical role in enhanced invasiveness of the multidrug resistant human breast cancer cells. J Proteome Res 2009;8:5041–7.
34. Hresko RC, Mueckler M. mTOR.RICTOR is the Ser^{473} kinase for Akt/protein kinase B in 3T3-L1 adipocytes. J Biol Chem 2005; 280:40406–16.
35. Guo H, Gu F, Li W, et al. Reduction of protein kinase Cζ inhibits migration and invasion of human glioblastoma cells. J Neurochem 2009;109:203–13.
36. Kay RR, Langridge P, Traynor D, Hoeller O. Changing directions in the study of chemotaxis. Nat Rev Mol Cell Biol 2008;9:455–63.
37. Ridley AJ, Schwartz MA, Burridge K, et al. Cell migration: integrating signals from front to back. Science 2003;302:1704–9.
38. Masri J, Bernath A, Martin J, et al. mTORC2 activity is elevated in gliomas and promotes growth and cell motility via overexpression of rictor. Cancer Res 2007;67:11712–20.